Strong x-ray magnetic circular dichroism in a "forbidden geometry" observed via photoemission

C. M. Schneider
Institut für Experimental Physik, Freie Universität Berlin, D-1000 Berlin 33, Germany

D. Venus
Physics Department and Institute for Materials Research, McMaster University, Hamilton, Canada L8S 4M1

J. Kirschner
Institut für Experimental Physik, Freie Universität Berlin, D-1000 Berlin 33, Germany
(Received 5 August 1991)

A strong magnetic circular dichroism has been observed in core-level photoemission in a geometry where it is considered to be forbidden—that is, when the x-ray wave vector and the sample magnetization vector are perpendicular. This observation is in sharp contradiction to existing models of circular magnetic dichroism. Recent experiments studying the $2p$ levels of iron indicate that a consistent interpretation of all the results is obtained when the final-state-selection effects of angle-resolved photoemission are taken into account.

Over the past few years, x rays have become an increasingly important probe of the magnetic properties of materials. There are a number of experimental arrangements where the cross section for the interaction of x rays and a solid depend on its local or global magnetic state.[1-3] Measurements of the relative changes in these cross sections, as the x-ray polarization or the sample magnetization is changed, produces an intensity asymmetry which can give insight into the presence, size and orientation of the magnetization. This effect is called magnetic dichroism. A subset of these experiments are performed using circularly polarized x rays, and display magnetic circular dichroism. Thus far, most of these experiments have been measurements of transmission, fluorescence, or total electron yield at absorption edges. In itinerant ferromagnets,[3-6] an independent electron model of absorption has proved adequate to understand magnetic circular dichroism at the K and L absorption edges. In localized magnetic systems, a correlated-hole model with explicit many-particle interactions is more appropriate.[7,8] Recently, x-ray magnetic circular dichroism has also been observed in core-level photoemission into unbound states far above the Fermi level.[9,10] The present understanding of this effect is also based on absorption models[9,11,12] which calculate the total yield as a function of the photoelectron energy.

All these experiments are similar in that the magnetic circular dichroism is dependent on the interaction of spin-orbit coupling and a magnetic exchange field. The exchange field defines an axis of spin quantization, and is accompanied by a spin-dependent, energetic splitting of states that would otherwise be degenerate. Each resulting state thus has a preferred spin orientation. The circularly polarized light defines a preferred orbital orientation through the dependence of the photoexcitation probabilities on the x-ray helicity. The role of spin-orbit coupling is to link these two independent, orientations. Magnetic circular dichroism arises from the difference in the photoexcitation probabilities when these two mechanisms "agree" or "disagree" on which is the preferred orientation along a common quantization axis. The important differences between the various experiments lie in whether the principal effects of the spin-orbit coupling and/or exchange field are manifest at the core energies, at the valence energies, or at both.

In all cases, the circular dichroism should disappear if the quantization directions selected by the exchange field and light helicity are orthogonal. Thus, in a ferromagnet, some component of the helicity (or, equivalently, the unit vector $\hat{\mathbf{q}}$ in the direction of light propagation) must be along the magnetization direction $\hat{\mathbf{M}}$,[3,9,11-13]

$$\hat{\mathbf{q}}\cdot\hat{\mathbf{M}}\neq 0 \ . \tag{1}$$

Despite this, recent experiments show a strong x-ray magnetic circular dichroism in core-level photoemission, even in the "forbidden" geometry when Eq. (1) is an equality. These experiments were performed at the BESSY synchrotron ring using the SX-700-II monochromator.[14] The x-rays provided by this monochromator are elliptically polarized, and can have a high degree of circularity if only a portion of the synchrotron beam is accepted, but it is not possible to reverse the sense of ellipticity. Measurements of the beam position in the monochromator indicate that a large component of circularly polarized light with negative helicity is present, but it is difficult to estimate the degree of ellipticity. The experimental geometry is illustrated in Fig. 1. The sample was a (110)-oriented iron single crystal that was remanently magnetized along the [001] direction in the crystal surface. The light was incident normal to the crystal surface and the magnetization, so that the angle $\theta-\beta$ in Fig. 1, was 90°. (θ is the angle between $\mathbf{q}$ and the emission direction.) The photoelectrons were collected at an angle $\beta=45°$ from the direction of magnetization, in the plane containing $\mathbf{q}$ and $\mathbf{M}$. This direction is close to the [111] crystalline direction. A hemispherical electron energy

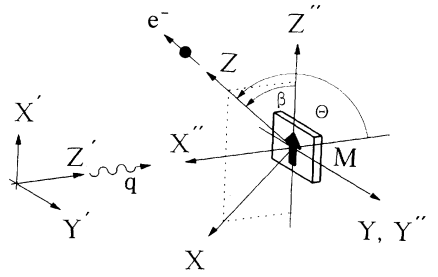

FIG. 1. The geometry of the experiments, and the subsequent calculations. The coordinate system $\mathbf{x}'',\mathbf{y}'',\mathbf{z}''$, is fixed to the crystal, with the polar axis determined by the direction of the magnetization, $\mathbf{M}$. The coordinate system for the incident light, $\mathbf{x}',\mathbf{y}',\mathbf{z}'$, has its polar axis defined by the light wave vector $\mathbf{q}$. The coordinate system $\mathbf{x},\mathbf{y},\mathbf{z}$ has its polar axis defined by the direction in which the photoelectrons are detected. θ is the angle between the light wave vector and emission direction, and β is the angle between the magnetization and emission direction.

analyzer with angle-resolving input optics was used. The data were obtained using a constant photon energy of 886 eV, and scanning the final state kinetic energy. The photoelectron intensity asymmetry was formed from two spectra taken with opposite senses of magnetization.

Representative data are shown in Fig. 2(a). The solid line is the sum of intensities for both magnetization directions as a function of photoelectron energy. The intensity asymmetry is plotted below, without any correction for background or the mixed polarization of the light. In Fig. 2(b), the data of Baumgarten *et al.*[9] are reproduced. This experiment on the same crystal had $\beta=55°$, and the light was incident at a glancing angle of $\theta-\beta=10°$. Thus $\hat{\mathbf{q}}$ had a large component along $\hat{\mathbf{M}}$ and the emission direction was almost exactly along [111]. The similarity between these curves is clear. Remarkably, the data taken at normal incidence,with $\hat{\mathbf{q}}\cdot\hat{\mathbf{M}}=0$, show a peak-to-peak asymmetry of 10% at the $p_{3/2}$ feature, which is more than twice as large as that observed in the earlier reports, when $\hat{\mathbf{q}}\cdot\hat{\mathbf{M}}$ was large.[15]

The origin of the contradiction to Eq. (1) is found in the difference between angle-integrated and angle-resolved photoemission. In the following, an independent electron model is used, although a similar calculation could be made using a correlated-hole model with many-particle interactions.[12] Much may be learned by refining the original calculation of magnetic circular dichroism in core levels by Erskine and Stern.[16] Since only photoelectrons emitted in a certain direction are detected, more attention must be given to specifying the final electronic state. The important observation is that in the photoexcitation matrix elements

$$M_{\rm fi}=\langle\Psi_f(\Omega)|O_h(\Omega')|\Psi_i(\Omega'')\rangle\delta(E_f-h\nu-E_i)\ , \qquad (2)$$

the coordinate systems (denoted by the different solid angles Ω, Ω', and Ω'') in which the dipole operator O_h and wave functions Ψ are naturally expressed, are different. These coordinate systems are illustrated in Fig. 1. Because of the strong spin-orbit coupling in the localized initial $2p$ states, these electronic states can be represented by atomic states whose angular variation is given by[17]

$$\chi_\kappa^\mu(\Omega'')=\sum_m C(l,\tfrac{1}{2},j;m,\mu-m)Y_{l,m}(\Omega'')|\mu-m\rangle\ . \qquad (3)$$

Here κ is a collective index for both l and j. $\kappa=1$ for the $p_{1/2}$ state and $\kappa=-2$ for the $p_{3/2}$ state, and μ is the azimuthal quantum number m_j. The Pauli spinor $|\sigma\rangle$ has its axis of quantization along the sample magnetization, and the spherical harmonic has it polar axis along $\mathbf{z}''$, parallel or antiparallel to $\mathbf{M}$. To first order, these states have an energy splitting proportional to μ in the exchange field $\mathbf{M}$.[18] Thus the energy of the state denoted by μ in a field $\mathbf{M}$, is equal to the energy of the state denoted by $-\mu$ in a field $-\mathbf{M}$. The photoexcitation probabilities with circularly polarized light, however, are different for $\pm\mu$. This is the origin of the dichroic asymmetry.[11]

The dipole operator $O_h(\Omega')$ for circularly polarized

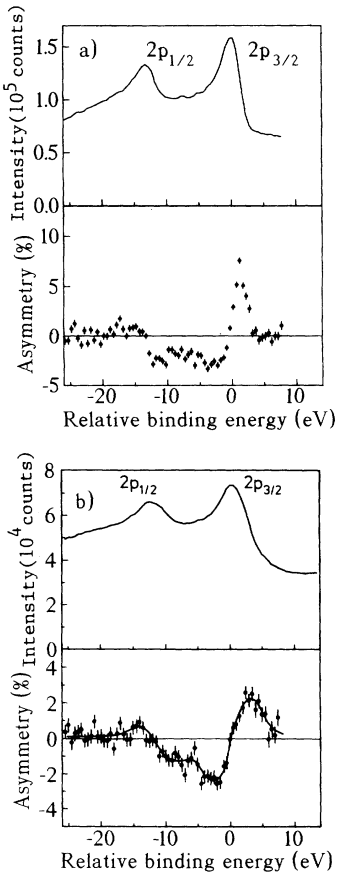

FIG. 2. (a) The upper curve shows the energy spectrum for photoexcitation of the $2p_{3/2}$ and $2p_{1/2}$ core levels of iron as a function of the binding energy. The light is normally incident on the (110) crystal face, and has wave vector $\mathbf{q}$ perpendicular to the sample magnetization $\mathbf{M}$ (which is along [001]). Photoelectrons are collected at 45° to the surface normal, in the plane defined by $\mathbf{q}$ and $\mathbf{M}$. The spectrum is the sum of two spectra taken with $\mathbf{M}$ in opposite directions. The lower curve is the intensity asymmetry obtained by taking the difference of the spectra for $\pm\mathbf{M}$ and dividing by their sum. (b) As in (a), except that the data is reproduced from Ref. 9. The light now has a glancing angle of incidence on the crystal, but the crystallographic direction of electron emission is very nearly the same.

light of helicity $h=m$ is represented by the spherical harmonic[17] $-mY_{1,m}(\Omega')$, where the polar axis is along z', parallel to q. For the final states in the three-step photoemission model, band states with a polar axis along the emission direction, z, are used. This is because, in an angle-resolved experiment, it is the symmetry operations with respect to the emission direction which determine which wave functions are coupled to the plane-wave states at the detector. The three-step model is adequate in the present case, since surface transmission effects cannot give rise to an intensity asymmetry for emission in a mirror plane.[19]

The changes in the matrix element due to the radial part of the wave function are ignored, since they are expected to be small and regular. Transitions to *s*-like states are also neglected in comparison to those to *d*-like states. This results in a series of angular matrix elements of the form

$$M^{m'}_{m,m''}=\langle Y_{2,m}(\Omega)|Y_{1,m'}(\Omega')|Y_{1,m''}(\Omega'')\rangle \ . \tag{4}$$

Transformation matrices are used to express all quantities in terms of the final-state reference frame. The matrix elements can be evaluated using Clebsch-Gordan coefficients and the appropriate sums are made over the initial spin states in Eq. (3), and the spherical harmonics in the final states (to obtain the correct spatial symmetry). The square modulus of the matrix elements is evaluated for emission angles β and $\beta+\pi$ to represent a reversal of magnetization, and the (μ,κ)-resolved (i.e., energy-resolved) intensity asymmetry is calculated.

Explicit calculation shows that the numerator of the expression for the dichroic asymmetry, A, for any linear combination of final states derived from *d* wave functions, can be expressed as a sum of two terms:

$$A\sim\hat{\mathbf{q}}\cdot\hat{\mathbf{M}}+(\hat{\mathbf{q}}\cdot\hat{\mathbf{z}})(\hat{\mathbf{z}}\cdot\hat{\mathbf{M}}) \ , \tag{5}$$

where numreical prefactors have been omitted. Thus it is clear that the emission direction plays an important "transference" role. Using as an analogy a phenomenon seen with linearly polarized light, the emission direction $\hat{\mathbf{z}}$ in the second term of Eq. (5) acts like an intermediate linear polarizer between crossed linear polarizers—it allows some light to pass due to a mutual projection along an intermediate axis. As a result, the present angle-resolved photoemission experiments continue to show a dichroic asymmetry even when the light is incident perpendicular to the magnetization. In an angle-integrated experiment, such as an absorption or total-yield measurement, the second term in Eq. (5) sums to zero, so that Eq. (1) is recovered.

As a semiquantitative application, consider the magnetic circular dichroism $A^{m'}_{m}(\mu,\kappa)$, for the $p_{1/2}$ peak, when circularly polarized light of negative helicity is used. For emission in the [111] direction in a mirror plane, only the final states transforming as $\Lambda_1\sim Y_{2,0}(\Omega)$ have the proper reflection symmetry in the three-step model.[20] Using only the transition probabilities, without appropriate lifetime or instrumental broadening, yields a maximum asymmetry of

$$A_0^{-1}(\mu,1)=\mathrm{sgn}(\mu)[4(\hat{\mathbf{q}}\cdot\hat{\mathbf{M}})-6(\hat{\mathbf{q}}\cdot\hat{\mathbf{z}})(\hat{\mathbf{z}}\cdot\hat{\mathbf{M}})]/[2+3\sin^2\theta] \tag{6}$$

for $\mu=\pm\frac{1}{2}$. In the present experimental geometry, this gives -0.86, whereas for the previous experiment at glancing incidence[9] (the emission direction with respect to the crystal differs by only 10°), the predicted asymmetry is -0.56. This ratio of approximately 1.5 between the two geometries is maintained, even if broadening is applied to the calculation. The results for the $p_{3/2}$ peak give essentially the same ratio of asymmetries in the two geometries[21] (however, the sign of both asymmetries is reversed). Because of background corrections, and the uncertainty in the relative degrees of circular polarization, these calculated dichroic asymmetries cannot be compared directly to the experiments, but it is significant that an asymmetry of the same (correct) sign and of significantly larger magnitude is predicted for the situation where $\hat{\mathbf{q}}\cdot\hat{\mathbf{M}}=0$, as is seen experimentally. This comes about because the second term in Eq. (6) is large and negative (even though the first term is zero), whereas in the experiment at glancing incidence, the first term is large and positive but the second term is also positive and must be subtracted off. It is therefore clear that the sign of the dichroic asymmetry must be interpreted with care, as it is not always given by the relative alignment of the photon helicity and sample magnetization. Other predictive and explanatory aspects of this simple model are the subject of a forthcoming publication.[22]

In conclusion, there are important differences between circular magnetic dichroism in x-ray core-level photoabsorption and angle-resolved photoemission. The absorption experiment is easier to perform, but, since it measures an integrated quantity, it yields less information than the angle-resolved photoemission experiment. The extra term in the magnetic circular dichroism can be exploited in a number of ways. Most fundamentally, it must be included to properly interpret the sign of the observed dichroism. Next, it makes it possible to search for an experimental geometry with a large asymmetry, so that further applications of the technique will be simpler. The present experiments show an increased magnetic dichroism in the favorable geometry of normal light incidence, where complications involving light depolarization at the surface and definition of the light spot on the crystal are minimized. The extra term can also provide sensitivity to both planar components of the magnetization (as well as any normal component). A fine discrimination between the behavior of the two terms in Eq. (5) can be made by simultaneous measurement of the dichroism in the angle-resolved photoemission and the total photocurrent. This technique could be used to determine the magnetization direction in the crystal plane without

the need for sample rotation. These capabilities are of particular utility for studying magnetic orientation in thin films, the magnetic coupling between a thin film and a substrate, or in imaging ferromagnetic domains with a photoemission microscope.

D. V. wishes to acknowledge partial support by the Natural Sciences and Engineering Research Council of Canada, and the Deutsch Forschungsgemeinschaft, which has allowed him to participate in these experiments. This work was supported by the Bundesminister für Forschungs und Technologie under Contract No. 05 413 AXI, TP 06.

[1]B. T. Thole, G. van der Laan, and G. A. Sawatzky, Phys. Rev. Lett. **55**, 2086 (1985).

[2]J. P. Hannon, G. T. Trammell, M. Blume, and D. Gibbs, Phys. Rev. Lett. **61**, 1245 (1988).

[3]C. Brouder and M. Hikam, Phys. Rev. B **43**, 3809 (1991).

[4]G. Schütz, W. Wagner, W. Wilhelm, P. Kienle, R. Frahm, and G. Materlik, Phys. Rev. Lett. **58**, 737 (1987).

[5]H. Ebert, P. Strange, and B. L. Gyorffy, Z. Phys. B **73**, 77 (1988).

[6]C. T. Chen, F. Sette, Y. Ma, and S. Modesti, Phys. Rev. B **43**, 7262 (1990).

[7]G. van der Laan, B. T. Thole, G. A. Sawatzky, J. B. Goedkoop, J. C. Fuggle, J. -M. Esteva, R. Karnatak, J. P. Remeika, and H. A. Dabkowska, Phys. Rev. B **34**, 6529 (1986).

[8]J. B. Goedkoop, B. T. Thole, G. van der Laan, G. A. Sawatzky, F. M. F. de Groot, and J. C. Fuggle, Phys. Rev. B **37**, 2086 (1988).

[9]L. Baumgarten, C. M. Schneider, H. Petersen, F. Schäfers, and J. Kirschner, Phys. Rev. Lett. **65**, 492 (1990).

[10]L. Baumgarten, S. Yumoto, C. M. Schneider, J. Kirschner, H. Petersen, and F. Schäfers, unpublished.

[11]H. Ebert, L. Baumgarten, C. M. Schneider, and J. Kirschner, Phys. Rev. B **44**, 4406 (1991).

[12]G. van der Laan, Phys. Rev. Lett. **66**, 2527 (1991).

[13]P. Carra and M. Altarelli, Phys. Rev. Lett. **64**, 1286 (1990).

[14]H. Petersen, Nucl. Instrum. Methods A**246**, 260 (1986).

[15]To some extent, the larger asymmetry can be attributed to better energy resolution. However, when the present data are artificially broadened by convolution with a Gaussian, a peak-to-peak asymmetry of 6% persists at a resolution comparable to the data of Ref. 9.

[16]J. L. Erskine and E. A. Stern, Phys. Rev. B **12**, 5016 (1975).

[17]M. E. Rose, *Elementary Theory of Angular Momentum* (Wiley, New York, 1957).

[18]H. Ebert, J. Phys. Cond. Matter **1**, 9111 (1991).

[19]R. Feder, in *Polarized Electrons in Surface Physics,* edited by R. Feder (World Scientific, Singapore, 1985).

[20]In the one-step photoemission model, the symmetry of the total system is only that of a mirror plane, so contributions from any symmetric combination $(Y_{2,m}+Y_{2,-m})$ could, in principle, be present and add coherently. These effects are expected to be small for large kinetic energies of the photoelectron, and cannot lead to an intensity asymmetry (see Ref. 19).

[21]For the $p_{3/2}$ peak, the asymmetry in the $|\mu|=\frac{1}{2}$ and $|\mu|=\frac{3}{2}$ states is different, so lifetime broadening must be applied in order to arrive at a single value for the maximum asymmetry. Again, the ratio of the maximum asymmetries for the two geometries is nearly independent of the details of the broadening or the value of the exchange splitting.

[22]D. Venus, C. M. Schneider, L. Baumgarten, C. Boeglin, and J. Kirschner, unpublished.